

Study of MWCNT/SnO₂ Nanocomposite Acetone and Toluene Vapor Sensors

Vladimir M. Aroutiounian, Zaven N. Adamyan, Artak G. Sayunts,
Emma A. Khachatryan, Arsen Z. Adamyan

Department of Physics of Semiconductors and Microelectronics, Center of Semiconductor Devices and Nanotechnologies, Yerevan State University, 1, A. Manoukian, 0025 Yerevan, Armenia,
Corresponding author's e-mail address: zad@ysu.am

Abstract

Thick-film acetone and toluene vapor sensors based on ruthenated multi-walled carbon nanotubes coated with tin-dioxide nanoparticles nanocomposite structures (MWCNTs/SnO₂) are prepared using three methods: hydrothermal synthesis, sol-gel technique and their combined method. It is shown that the optimal conditions for applications as acetone and toluene as well as ethanol and methanol vapors sensors in view of high response and selectivity relative to each other depend on choice of material synthesis method, mass ratio of the nanocomposite components and selected operating temperature. MWCNTs/SnO₂ sensor structures having the mass ratio of the components 1:4 and 1:24 exhibit selective sensitivity to acetone and toluene vapors at 150°C operating temperature, respectively. The samples with 1:200 mass ratio of the nanocomposite components was shown the selective response to acetone vapors exposure in the range of 200-250°C operating temperatures. The high sensitive and selective response to ethanol and methanol vapors is typical for the sensor structures made by different methods with the 1:8, 1:24, 1:50 and 1:66 mass ratio of the components, respectively, only at 200°C operating temperature. The dependence of the gas response vs acetone and toluene vapor concentration is linear beginning from 100 ppm and higher.

Key words: MWCNTs/SnO₂, VOCs, sensor, acetone, toluene.

1. Introduction

Advancement of the sensing technology is generated a need of mankind safety and security as well as monitoring of air pollution. So, air pollution influences human health and can cause a number of diseases. The main air pollutants are some inorganic gases as well as various volatile organic compounds (VOCs). Among others, toxic and pollutant VOCs such as acetone and toluene are found in indoors. The main sources the same VOCs in outdoor are industrial emissions combustion processes, traffic vehicles and fuel evaporation [1]. Since, the probability of over exposure to these contaminants now is very high, gas sensing devices installation in such places and develop of advanced monitoring systems for their early detection are necessary.

Acetone widely used in industries and labs. It is extensively used to dissolve plastic, purify paraffin, and dehydrate tissues in pharmaceuticals. Inhalation of acetone causes headache, fatigue and even narcosis and harmfulness to nerve system. Acetone is other important VOCs in breath. Highly sensitive acetone gas sensors are essential for identification of diabetes and monitoring health

conditions and treatment of diabetic patients [2]. The rapid and sensitive analysis of acetone gas concentration in human breath is a key technique for noninvasive diagnosis of diabetes. The traditional gas chromatography system as well as calorimetric and optical methods or some others used for this purpose is expensive and requires special knowledge for operation, which is not suitable for real-time measurements.

Gas sensors based on nanostructured semiconductor metal-oxides materials such as nanoparticles, nanowires, nanobelts, polycrystalline nanotubes, nanorods, hollow spheres and others or their nanocomposites with carbon nanotubes (CNTs) [3-6] are considered as the most promising for applications in gas detection systems and devices. In itself, CNTs possess by a number of useful behaviors such as a wide range of electrical properties, small size, high structural and chemical stability, high strength and so on. Dew to introduction of CNTs to metal-oxide matrix or deposition of metal-oxide nanoparticles on the nanotubes walls, specific surface area of such gas-sensitive nanocomposites increases still more. Moreover, additional nanochannels in the form of hollow

CNTs for gas diffusion appear [7]. Hence, it can be expected that application of nanocomposite hybrid structures composed of functionalized CNTs and metal oxide in gas sensors technology should improve the gas sensor parameters, particularly, gas sensitivity, response and recovery times as well as reduce the operating temperatures.

As a gas-sensitive materials meant for use in high performance gas sensor applications both taken separately and as a component of hybrid system, researches have mainly focused their efforts on n-type nanostructured metal-oxides such as SnO₂, In₂O₃, ZnO, WO₃, TiO₂ and their compounds [3-8]. Among them, SnO₂ is the most prospective and widely used gas-sensitive material for the gas sensor to detect a wide variety of pollutant gases due to its advantages and attractive features including high gas sensitivity, relatively low specific resistance and operating temperatures, chemical durability, low cost, nontoxicity and simple processing [9].

In previous work [4], we had shown that the functionalization of multi-walled carbon nanotube (MWCNT)/SnO₂ thick-film structures by Ru leads to considerable increase in response signal to methanol and ethanol vapors as well as to i-butane gas. However, the selectivity problem of studied sensors relative to other gases, particularly to some harmful and toxic VOCs exposure remained not solved. The goal of present work is bring to light on optimal conditions at which the best level of the selectivity these sensors to various VOCs including acetone and toluene vapors achieves. In this paper, we report the acetone and toluene sensing properties of various ruthenated MWCNT/SnO₂ nanocomposite structures as thick films obtained by hydrothermal synthesis and sol-gel techniques as well as their combination. The choice of corresponding treating conditions and regimes for CNTs functionalization as well as thick films surface modification with Ru catalyst were focused on obtaining sensitivity to mentioned target gases.

2. Experimental

2.1. Materials preparation

MWCNTs/SnO₂ nanopowders for thick film preparation were made by the following three ways: using sol-gel preparation technique, hydrothermal synthesis and their two-step combination.

To making the nanocomposite structures according to the first way, MWCNTs membranes (kindly provided us by our colleagues from University of Szeged, Hungary) were used for preparation of nanocrystalline MWCNTs/SnO₂ powder. For a functionalization of nanotube walls with oxygen-containing

hydroxyl (OH), carbonyl (C=O), and carboxylic (COOH) functional groups, MWCNTs from the membranes were transferred to slurry in HNO₃/H₂SO₄ acids mixture during 1 h. Such a functionalization of the CNTs is very important and necessary for the following synthesis of SnO₂ nanoparticles on the MWCNTs walls since these oxygen-containing groups act as sites for nucleation of nanoparticles. After rinsing by distilled water and drying at 80 °C MWCNTs were poured and treated in deionized water in ultrasonic bath for 5 min.

The sol-gel as well as hydrothermal synthesis processes are presented elsewhere [4], in detail. The final mass ratios of the MWCNT/SnO₂ nanocomposite obtained with a hydrothermal method were 1:4, 1:8, 1:66, and 1:200, respectively but one with a sol-gel method was 1:50.

The third type of composite material using both hydrothermal and wet chemical methods was obtained by following route. Firstly, we were prepared 45 ml 0.5M SnCl₄ · 5H₂O deionized water solution. Then, 11 mg hitherto obtained MWCNT/SnO₂ powder synthesized by above-mentioned hydrothermal method was added to the solution with thorough mixing by magnetic stirrer. Simultaneously, ammonium was added drop by drop to the solution at 42 °C on reaching pH=9. After that, the solution was left in the thermostat at 80 °C for 24 hours. Resulting slurry with deionized water addition was centrifuged at a spinning rate of 7000 rpm with further washing of the precipitates. Spinning and washing processes were carried out as long as chlorides in the solution disappear entirely. Then, the purified from chlorides sediment was left at 140 °C overnight. Obtained powder was annealed in air at 400 °C for 3 hours. The final mass ratio of obtained by such a way MWCNTs/SnO₂ composite components was 1:24, respectively.

The chose water as a solvent, instead of e.g. ethanol, in all presented here three material preparation methods was preferably for us in the view of expected improvement in gas sensing characteristics, taking in account the fact that cover the overwhelming parts of CNTs with SnO₂ nanoparticles is ensured at that [10].

2.2. Samples

The thick films were obtained on the base of all MWCNTs/SnO₂ composite powders. The paste for thick film deposition made by mixing powders with α-terpineol ("Sigma Aldrich") and methanol was printed on chemically treated surface of the alumina substrate over the ready-made Pt interdigitated electrodes. The thin-film Pt heater was formed on the back side of the substrate. Obtained composite structures were cut into 3×3 mm pieces. Drying and annealing

of the resulting thick films were carried out in two stages: heating up to 220°C with 2°C min⁻¹ rate of temperature rise, hold this temperature for 3 h and then further temperature increase until 400°C with 1°C min⁻¹ rate and hold again for 3 h. Then, the thick-film specimens were cooled down in common with the oven.

After annealing and cooling processes, the MWCNTs/SnO₂ thick films were surface-ruthenated by dipping them into the 0.01 M RuO₄ aqueous solution for 20 min whereupon dried at 80°C for 30 min and then annealing treatment was carried out again at the same above-mentioned mode. The choice of the ruthenium as a catalyst was defined by its some advantages [4]. Further, ruthenated MWCNT/SnO₂ chips were arranged in TO-5 packages and after leads bonding offered gas sensors were ready to measurements.

2.3. Gas sensing measurements

VOCs vapors sensing properties of the MWCNTs/SnO₂ composite structures were measured by home-made developed computer-controlled static gas sensor test system [11]. The sensors were re-heated at different operating temperatures. When the resistances of all the sensors were stable, saturated target vapor was injected into a measurement chamber by a microsyringe. The target gases including acetone, toluene, ethanol and methanol vapors were introduced in the measurement chamber on special hot plate designed for the quickly conversion of the liquid substance to its gas phase. After the sensor resistances reached a new constant value, the test chamber was opened to recover the sensors in air. The sensing characteristics were studied at a temperature range of 100-300°C. The gas response of the sensors was defined as R_a/R_g where R_a and R_g are the electrical resistances in air and in target VOCs-air mixed gas, respectively. The response and recovery times are defined as the time required for reaching 90% resistance change from the corresponding steady-state value of the signal.

3. Results and discussions

3.1. Material characterization

The morphologies of the prepared SnO₂/MWCNT nanocomposite different powders were studied by scanning electron microscopy (SEM) using Hitachi S-4700 Type II FE-SEM equipped with a cold field emission gun operating in the range of 5–15 kV. Results of these investigations presented elsewhere [4] in detail. There, we were shown that with increasing the mass ratio of the MWCNT/SnO₂ nanocomposite components from 1:4 to 1:200 the inorganic coverage of carbon nanotubes becomes thicker and thicker.

The presence of an oxide layer was confirmed by SEM-EDX and the crystalline structure of the inorganic layer was also studied by an X-ray diffraction method using Rigaku Miniflex II diffractometer (angle range: $2\theta [^\circ] = 10-80$ utilizing characteristic X-ray (CuK α) radiation). Results of these studies are presented in [4]. Here, we are only noted that the average crystalline size of SnO₂ nanoparticles is less than 12 nm for all used synthesis methods.

3.2. Gas sensing characteristics

For clarity sake, codes of studied at our view the most prospective acetone and toluene vapors sensitive samples and their corresponding synthesis methods as well as mass ratios of the nanocomposite components are summarized in Table 1 below.

Table 1: Designations of the samples and theirs corresponding process parameters

| Sample code | Process parameters |
|-------------|-------------------------------|
| KCS1-3 | Hydrothermal synthesis, 1:4 |
| EKCS3-2 | Hybrid method, 1:24 |
| ECS7-2 | Sol-gel technique, 1:50 |
| ZCS-200 | Hydrothermal synthesis, 1:200 |

It should be noted that 200°C is optimal operating temperature for detection of methanol and ethanol vapors by such nanocomposite sensors [4]. But, we were set ourselves as an object to find conditions and corresponding material technology at which the best selectivity to one or another gases achieves. With this purpose, we were carried out the testing of all samples at different operating temperatures in order to compare responses to various considered here target VOCs.

Taking into account the fact that KCS1-3 set of samples with 1:4 mass ratio of the nanocomposite components also selectively sensitive to methanol and ethanol vapors exposure at 200°C but with lesser responses in comparison with samples distinctive by own higher ratio of the components, we were hoped obtaining selective sensitivity KCS1-3 samples to acetone or toluene vapors at lower or higher operating temperatures. The responses of KCS1-3 samples to studied VOCs vs operating temperature is presented in Fig. 1. It can be seen that the selective sensitivity these samples to acetone vapors at the same concentration of all vapors is observed as early as at 150°C operating temperature. With increase in operating temperature, the response to acetone vapor rises up to 360.4 value at 250°C while the selectivity remains sufficiently high. Undoubtedly, functioning at lower operating temperature (150°C) with

ensuring the best selectivity is preferably in all cases.

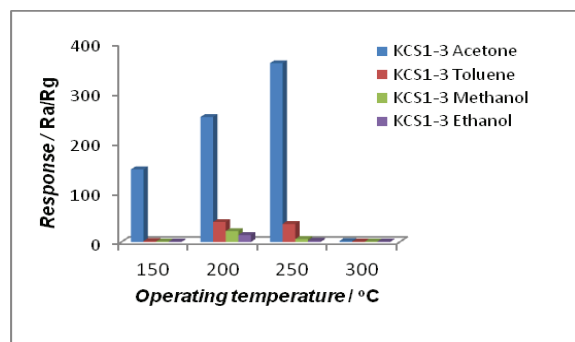


Fig. 1. The responses of specimens on KCS1-3 set of samples to studied VOCs exposure vs operating temperature.

As for EKCS3-2 set of samples made by applying of the hybrid technology, we should be noted that the high response to acetone and toluene vapors of these sensors appears at 200°C but selectivity at that is poor. The selective response to toluene vapors is observed at 150°C (Fig. 2). Thus, KCS1-3 and EKCS3-2 sets of samples functioned at relatively low operating temperature (150°C) could be use as toluene and acetone vapors selective sensors, respectively.

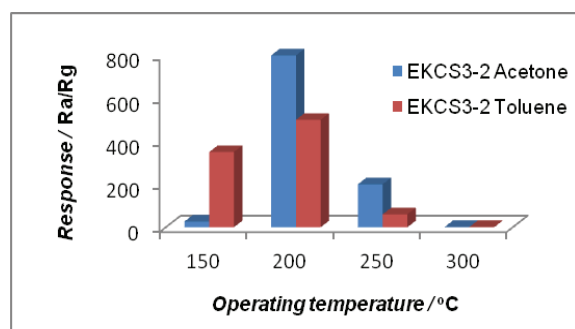


Fig. 2. The response of EKCS3-2 set of samples to the same concentration (500 ppm) of acetone and toluene vapors vs operating temperature.

The selective sensitivity to acetone vapors of ECS7-2 set of samples takes place at 300°C (Fig. 3). It should be noted that the same samples show very high response to ethanol and methanol (up to three orders of magnitude) at lower operating temperatures (see [4]).

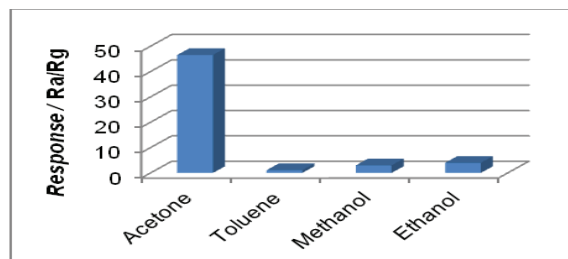


Fig. 3. Responses of ECS7-2 series samples to 1000 ppm of various VOCs at 300°C operating temperature.

Sufficiently selective response to acetone vapors is registered by ZCS1-200 set of samples at all operating temperatures in the range of 150-300°C. Results of the test measurements are shown in Fig. 4 and can find in the Table 2 where data of acetone and toluene responses of considered samples at different operating temperatures are summarized.

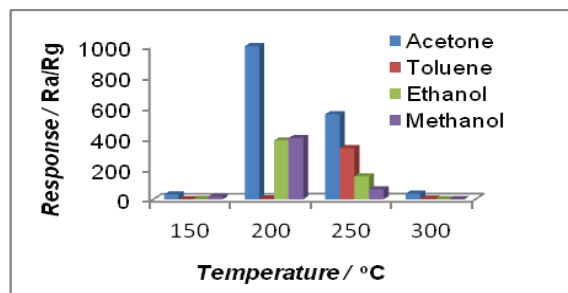


Fig. 4. The response of specimens on ZCS1-200 set of samples to 1000 ppm of studied VOCs exposure vs operating temperature.

Table 2. Acetone and toluene vapors responses of studied samples vs operating temperature.

| T / °C | Gas response, R_a/R_g | | | | | | | |
|--------|-------------------------|---------|---------|---------|---------|---------|----------|---------|
| | KCS1-3 | | EKCS3-2 | | ECS7-2 | | ZCS1-200 | |
| | Acetone | Toluene | Acetone | Toluene | Acetone | Toluene | Acetone | Toluene |
| 150 | 146.3 | 2 | 26.59 | 350 | 2.67 | 4.88 | 32.3 | 1 |
| 200 | 251.9 | 40.21 | 800 | 500 | 7.62 | 6.25 | 1002.34 | 5 |
| 250 | 360.4 | 84.198 | 200 | 60 | 86.93 | 52.96 | 555.6 | 334.6 |
| 300 | 2.21 | 1 | 1 | 1 | 46.5 | 1 | 37.5 | 4.34 |

Response and recovery times are defined from transient response-recovery curves and corresponding dynamic resistance change. As examples, here we adduce some of them for different mentioned above gas sensors. These times to differ for studied sensors. As can see from Fig. 5, the reaction of EKCS3-2 sensors to acetone vapors is rather slow. The recovery at 200°C takes place incompletely. Using pulse supply mode for heater full recovery is reached. But, response and recovery times, for example, of KCS1-3 type sensors at 250°C operating temperature and 1000 ppm toluene exposure are about only 24 s and 14 s, respectively (here corresponding response-recovery curve is not shown).

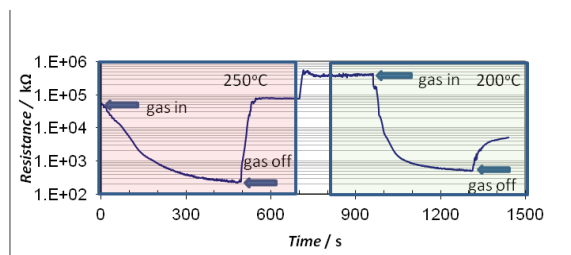


Fig. 5. The response and recovery of EKCS3-2 set of samples to 500 ppm acetone vapors exposure starting at 250°C and then 200°C operating temperatures.

The largest response to acetone vapors ($R_a/R_g=555,62$) in steady-state regime (formed after the first acetone vapor influence) is fixed for ZCS1-200 set of samples with 1:200 mass ratio of the components to 1000 ppm acetone vapors exposure at 250°C operating temperature (Fig. 6). Response and recovery times of these sensors are about 22 and 27 s, respectively.

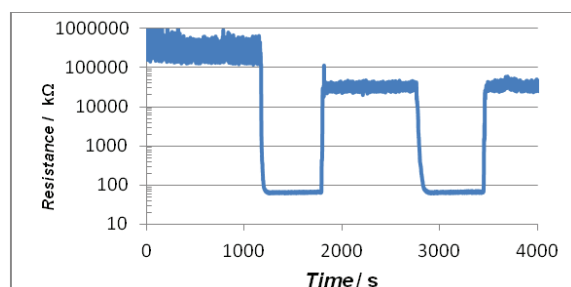


Fig. 6. The response and recovery of ZCS1-200 set of samples with 1:200 mass ratio of the components to 1000 ppm acetone vapors exposure at 250°C operating temperature.

As an example, dependence of EKCS3-2 sensors response vs acetone vapor concentration at 150°C is presented in Fig. 7. Here, the experimental curve in common with the corresponding measured response points

presents as blue color whereas black line shows fitting linear law. Obviously that the gas response linearly increases with the acetone vapor concentration build up.

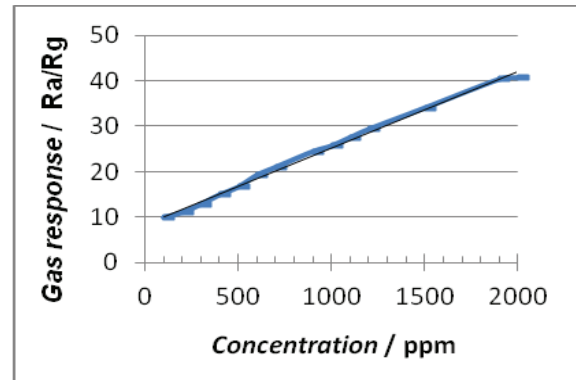


Fig. 10. Dependence of EKCS3-2 sensor response vs acetone vapor concentration.

Conclusion

Thus, in this work are found definite conditions at which of studied MWCNTs/SnO₂ nanocomposite gas sensors exhibit the selective reaction to acetone and toluene vapors. This one are achieved both by selection of samples with corresponding mass ratio of the nanocomposite components and choice of the optimal operating temperature for each set of samples. So, it is revealed that the nanocomposite structures with 1:4 mass ratio of the components selectively respond to acetone vapors at 150°C and acetone and toluene vapors at 250°C operating temperatures. Nanocomposite samples with greater mass ratio of the components (1:8, 1:24, 1:50, 1:66 and 1:200) behave as a very sensitive and selective ethanol and methanol sensors at 200°C operating temperature [4]. Acetone vapors selective sensitivity of samples with 1:50 mass ratio of the components appears only at 300°C operating temperature. The largest and sufficiently selective response to acetone vapors (R_a/R_g more than three orders of magnitude at 1000 ppm acetone vapor concentration) is achieved for samples with 1:200 mass ratio of the components. The dependence of the gas response vs acetone and toluene vapor concentration is linear beginning from 100 ppm and higher.

This work supported by NATO EAP.SFPF 984.587 and State Committee of Science MES RA 13-1C075 projects.

References

- [1] S. Gokhale, T. Kohajda, U. Schlink, *Source apportionment of human personal exposure to volatile organic compounds in homes, offices and outdoors by chemical mass balance and genetic algorithm receptor models*, *Sci. Total Environ.* 407, 122–138 (2008); doi: org/10.1016/j.scitotenv.2008.08.025
- [2] Xue Bai, Huiming Ji, Peng Gao, Ying Zhang, Xiaohong Sun, *Morphology, phase structure and acetone sensitive properties of copper-doped tungsten oxide sensors*, *Sens. Actuators B* 193, 100–106 (2014); doi: 10.1016/j.snb.2013.11.059
- [3] G. Korotcenkov, S.-D. Han, B.K. Cho, V. Brinzari, *Grain size effects in sensor response of nanostructured SnO₂- and In₂O₃-based conductometric thin film gas sensor*, *Critical Reviews in Solid State and Materials Sciences* 34, 1–17 (2009); doi: 10.1080/10408430902815725
- [4] V.M. Aroutiounian, A.Z. Adamyan, E.A. Khachaturyan, Z.N. Adamyan, K. Hernadi, Z. Pallai, Z. Nemeth, L. Forro, A. Magrez, E. Horvath, *Study of the surface-ruthenated SnO₂/MWCNTs nanocomposite thick-film gas sensors*, *Sensors and Actuators B* 177, 308–315 (2013); doi: org/10.1016/j.snb.2012.10.106
- [5] Sadegh Ahmadnia-Feyzabad, Abbas Ali Khodadadia, Masoud Vesali-Naseh, Yadollah Mortazavi, *Highly sensitive and selective sensors to volatile organic compounds using MWCNTs/SnO₂*, *Sensors and Actuators B* 166–167, 150–155 (2012); doi: 10.1016/j.snb.2012.02.024
- [6] N.V. Hieu, L.T.B. Thuy, N.D. Chien, *Highly sensitive thin film NH₃ gas sensor operating at room temperature based on SnO₂/MWCNTs composite*, *Sensors and Actuators B* 129 (2008) 888–895; doi:10.1016/j.snb.2007.09.088
- [7] Xue Bai, Huiming Ji, Peng Gao, Ying Zhang, Xiaohong Sun, *Morphology, phase structure and acetone sensitive properties of copper-doped tungsten oxide sensors*, *Sens. Actuators B* 193, 100–106 (2014); doi: org/10.1016/j.snb.2013.11.059
- [8] L. Wang, A. Teleki, S.E. Pratsinis, P.I. Gouma, *Ferroelectric WO₃ nanoparticles for acetone selective detection*, *Chem. Mater.* 20, 4794–4796 (2008); doi: 10.1021/cm800761e
- [9] G. Korotcenkov, S.H. Han, B.K. Cho, *Material design for metal oxide chemiresistive gas sensors*, *Journal of Sensor Science and Technology* 22(1), 1-17 (2013); doi.org/10.5369/JSST.2013.22.1.1
- [10] Z. Nemeth, B. Reti, Z. Pallai, P. Berki, J. Major, E. Horvath, A. Magrez, L. Forro, K. Hernadi, *Chemical challenges during the synthesis of MWCNT-based inorganic nanocomposite materials*, *Phys. Status Solidi B* 251, 2360-2365 (2014); doi: 10.1002/pssb.201451141
- [11] A.Z. Adamyan, Z.N. Adamyan, V.M. Aroutiounian, A.H. Arakelyan, J. Turner, K. Touryan, *Sol-gel derived thin-film semiconductor hydrogen gas sensor*, *Int. J. of Hydrogen Energy*, 32, 4101-4108 (2007); doi:10.1016/j.ijhydene.2007.03.043